

E. E. EL-Kholy  
A. EL-Sabbe  
S. S. Shokralla  
N. A. EL-Hefnawy

Electrical Engineering Department,  
Faculty of Engineering, Menoufiya  
University, Shebin El-Kom, Egypt.

J. Electrical Systems 1-1 (2005): 26-38

Regular paper

## **A Practical Fast Acting Control Scheme For Fuzzy Logic-Based Voltage Stabilization Control**



*Journal of  
Electrical  
Systems*

*This paper presents a simplified control model for stabilizing a load voltage using a switched reactor in parallel with a fixed capacitor of static VAR compensator. Two IGBT's are used to control the reactance of the switched reactor. A uniform pulse width modulation is used for controlling the two switches. The compensator has a simple control circuit and structure. A complete modeling and numerical simulation for the proposed systems is presented. A high speed Digital Signal Processor is used for implementing proportional-integral (PI) and fuzzy load voltage controllers. Experimental results indicate the superiority of fuzzy logic control over the conventional proportional-integral control method. Simulation results are reported and proved to be in good agreement with the relevant experimental results.*

**Keywords:** VAR compensator, Reactive power control, Load voltage stabilization, Fuzzy logic control.

### **1. INTRODUCTION**

In recent years, the demand for controllable reactive power source has gone up mainly for efficient and reliable operation of ac electric power system [1]. VAR compensators should be controlled to provide rapid and continuous reactive power supports during static and dynamic power system operating conditions [2]. Advances in power electronics technology have allowed the development of various types of controlled electronics VAR compensator for power system applications [3-4].

There have been several papers published regarding the use of shunt compensating capacitors with series harmonic suppressor inductors in power factor correction and terminal voltage stabilization of non-linear loads. There are various static VAR compensator topologies based on forced commutated voltage source inverter [5-12]. In reference [6], scheme uses a filter reactor on the line side and self-controlled dc bus. The modulation index is controlled directly by the VAR calculator. The scheme allows the use of optimized PWM patterns for harmonic rejection and is suitable for slowly varying VAR demand applications. In reference [7], the modulation index is fixed and the capacitor voltage is controlled so that the inverter output voltage matches in magnitude the line voltage. Capacitor voltage control is achieved through phase shifting of the inverter voltage with respect to the line voltage. In spite of its simplicity, the load angle control scheme does not allow very fast response to be achieved particularly at high power ratings. Thyristors controlled reactors are a source of harmonics distortion in power systems [7].

In reference [8], two filter arms are considered; one is tuned for third harmonic frequency and other is for the fifth one. These filters are used to eliminate the third and fifth current harmonics as well as reducing the terminal voltage distortion. Synchronous compensators, mechanically switched capacitors and inductor and saturated reactors have been applied for many years to control the system voltage. Also, thyristor controlled reactor (TCR) devices together with fixed capacitors (FC) or thyristor – switched capacitors (TSC) have been used. The rating of inductors and capacitor used in the TCR/FC or TCR/TSC scheme, in most cases, exceeds the reactive power supplied or absorbed by the scheme. This leads to considerable expenses and large requirement for land on which to locate the compensator [9]. Steady-state characteristics are reported for open loop systems for switch reactor based static VAR compensators [10]. In reference [11], a static reactive

power compensator is designed to be capable of supply both balanced and unbalanced reactive power demands. In reference [12], error-driven, error-scaled, self-adjusting SVC-control strategy is driven by the presence of a nonlinear dynamic loads. This control ensures adequate compensation level and damping effectiveness at all times based on the magnitude of the excursion error deviation-vector in the error hyperplane.

In this paper an efficient switched reactor in parallel with a capacitor for static VAR compensator is presented. To overcome the low-order harmonics and slow response associated with the conventional thyristor controlled reactor compensators, the uniform pulse width modulation is used for controlling the reactance of the switched reactor. The proposed system is implemented using a high speed digital signal processor (DSP) for PI and/or fuzzy logic load voltage controllers. The system behavior under steady-state and transient condition is obtained and proved the superiority of the fuzzy logic controller over the conventional PI controller method. There are agreement between the simulation and experimental results.

**2. DESCRIPTION OF THE SYSTEM**

The system under consideration is illustrated in Fig. 1. The system consists of two IGBT switches, one reactor, a fixed capacitor and load; all of them are in parallel. However, two self-commutated bi-direction IGBT switches are used to control the reactance of the switched reactor. The simulation and experimental results are verified using an inductive load and /or dynamic load. The source reactance is taken 15 % to 20 % of the load impedance and the source resistance is taken 10 % of the source reactance [8]. The values of the controlled reactance and capacitance of the compensator are selected according to the following relationship [8]:

$$C\omega = \frac{1}{\omega L_{\theta}} = \frac{1}{z_L} = \sin(\phi_1) \tag{1}$$

The parameter values of the designed system are given in the Appendix. The differential equations that describe the mode of operation for this system are given in reference [10]. The gate pulses are achieved by comparing the controller output with the triangular carrier signal using the DSP. The operation principle of the proposed system can be illustrated in Fig. 1. The two switches  $Q_1$  and  $Q_2$  represent two self-commutated bi-directional switches. Switch  $Q_2$  is used to freewheel the controlled inductor current ( $i_{L\theta}$ ) when  $Q_1$  is off. Through high frequency switching, the fundamental component of the inductor current ( $i_{L\theta}$ ) can be controlled by controlling the output, to stabilize the load voltage at constant value.

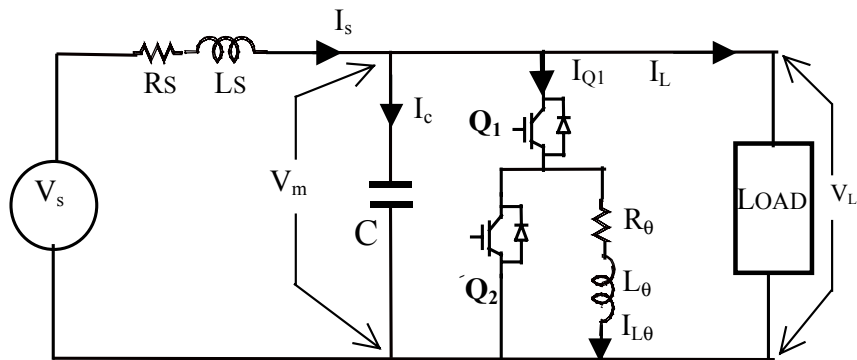


Fig. 1 Schematic diagram of proposed system.

### 3. FUZZY CONTROLLER FOR LOAD VOLTAGE STABILIZATION

The inputs of the fuzzy controller are the error  $e(k)$  and the change of error  $ce(k)$ , which are defined as:

$$e(k) = V_{ref} - V_m(k) \quad (2)$$

$$ce(k) = e(k) - e(k-1) \quad (3)$$

where  $V_m(k)$  is the present load voltage  $V_{ref}$ , is the reference voltage, and the subscript  $k$  denotes values taken at the beginning of the  $k^{th}$  switching cycle. The output of the fuzzy controller is the control voltage and is defined as:

$$V_c(k) = V_c(k-1) + \xi \Delta V_c(k) \quad (4)$$

where  $\Delta V_c(k)$  is the inferred change of control voltage by the fuzzy controller at the  $k^{th}$  sampling time, and  $\xi$  is the gain factor of the fuzzy controller. Adjusting  $\xi$  can change the effective gain of the controller.

The values of  $e(k)$ ,  $ce(k)$  and  $\Delta V_c(k)$  are normalized. The triangular shape of the membership functions of this arrangement presumes that for any particular input there is only one dominant fuzzy subset. Also for any combination of  $e$  and  $ce$ , a maximum of four rules are adopted.

The derivation of the fuzzy control rules is heuristic in nature and based on the following criteria:

- 1- when the load voltage of the common coupling bus-bar is far from the set point, the change of control signal must be large so as to bring the output to the set point quickly.
- 2- when the load voltage of the common coupling bus-bar is approaching the set point, a small change of control signal is necessary.
- 3- when the load voltage of the common coupling bus-bar is near the set point and is approaching it rapidly, the control signal must be kept constant so as to reduce overshoot.
- 4- when the set point is reached and the output input still changing, the control voltage must be changed a little bit to prevent the load voltage from moving away.
- 5- when the set point is reached and the load voltage is steady, the control voltage remains unchanged.
- 6- when the load voltage is above the set-point, the sign of the change of control voltage must be negative.
- 7- when the load voltage is below the set-point, the sign of the change of control voltage must be positive.

The inference result of each rule consists of two parts, the compatibility (weighting factor)  $w_i$  of the individual rule, and the degree of change of control signal  $C_i$  according to the rule. The weighting factor  $w$  is obtained by applying the minimum operation on the  $\mu(e_0)$  and  $\mu(ce_0)$ , where  $e_0$  and  $ce_0$  are the singleton inputs of  $e$  and  $ce$ .  $C_i$  is obtained from the rules, which show the mapping from the product space of  $e_0$  and  $ce_0$  to  $C_i$ . The inferred output of each rule can therefore be written as:

$$\Delta V_{ci} = \min \{ \mu_c(e_0), \mu_{ce}(ce_0) \} C_i = w_i C_i \tag{5}$$

where  $\Delta V_{ci}$  denotes the change of control signal inferred by the  $i^{\text{th}}$  rule. After collecting all the results, a crisp value of the change of control voltage can be obtained. Here the method of the center of gravity is preferred. The resultant change of control signal can be found as:

$$\Delta V_c(k) = \frac{\sum_{i=1}^N \Delta V_{ci}}{\sum_{i=1}^N w_i} = \frac{\sum_{i=1}^N w_i C_i}{\sum_{i=1}^N w_i} \tag{6}$$

where  $N$  is the maximum number of effective rules.

#### 4. SIMULATION AND EXPERIMENTAL RESULTS

The proposed system is designed and implemented using DSP to verify the load voltage control requirements with PI controller and/or fuzzy logic controller. The experimental set-up is shown in Fig. 2, the load is static and/or dynamic. A universal motor under test is coupled to a self-excited dc generator, which acts as a load. An incremental encoder is coupled to the motor shaft to measure the motor speed. The load, supply and compensator current are sensed using hall-effect transducers, which have good linear response over wide range. Also, the load and supply voltages are sensed using voltage transducer, which has good linear response over wide range. This system is fully controlled by using dSPACE (DS1102) controller board, which is installed on a PC computer.

The behavior of this system under steady state and transient conditions are obtained for static inductive load. The system has been tested using dynamic load, which is the universal motor. These results show the accuracy of the developed simulation when compared with the experimental results.

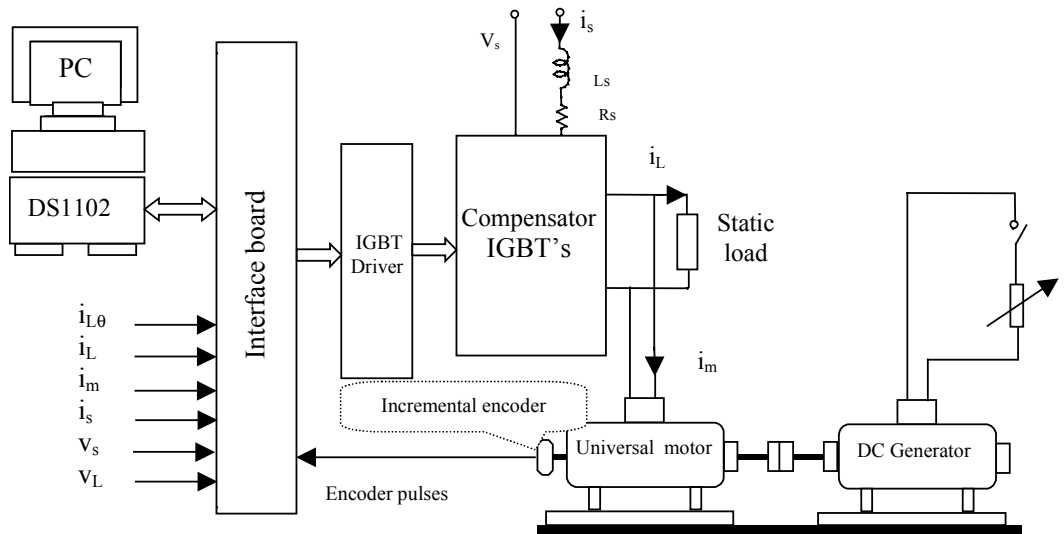


Fig. 2 Experimental set-up for DSP-based control

#### 4.1. Open-loop PI controller for static load

Figure 3 shows the experimental waveforms of the supply voltage ( $v_s$ ) and current ( $i_s$ ) with duty ratio equal to 0.7. It is observed that the power factor at common coupling bus-bar near unity power factor. Also, it is clear that the supply voltage and current waveforms are sinusoidal.

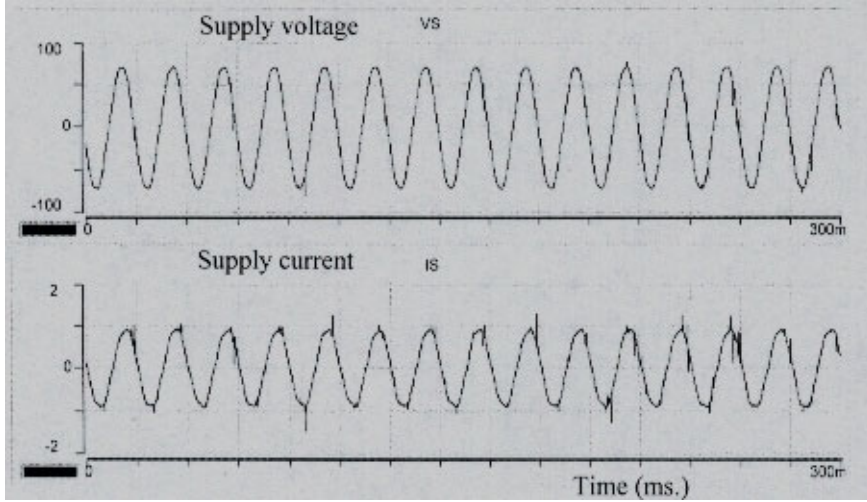


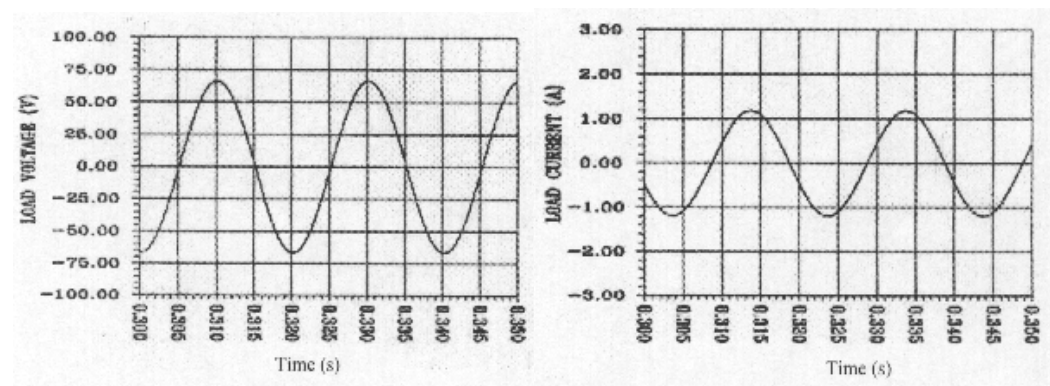
Fig. 3 Experimental waveforms for supply voltage and current.

Figure 4 shows the simulation and experimental waveforms of the load voltage ( $v_L$ ) and current ( $i_L$ ). It is noticed that the waveforms are sinusoidal. Figure 5 shows the experimental load voltage ( $v_L$ ), compensator inductor current ( $I_{L\Delta}$ ) and switch  $Q_1$  current ( $i_{Q1}$ ). It is observed that the inductor current lags the common coupling load voltage by  $90^\circ$ .

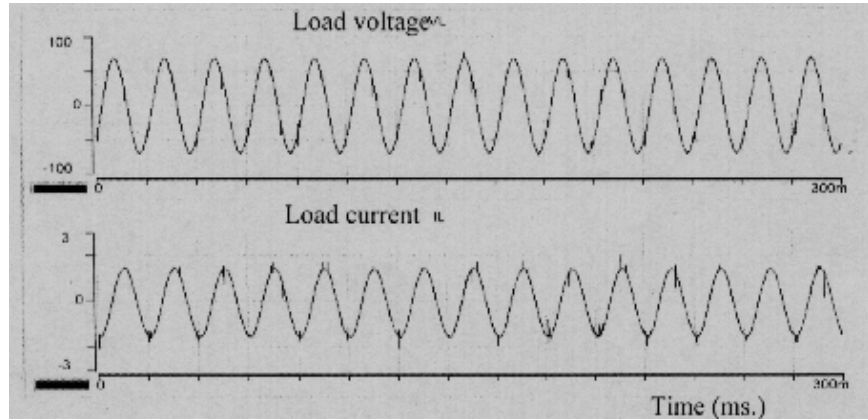
#### 4.2. Closed loop PI controller for static load

##### 4.2.1. Reference voltage step change

Figures 6 and 7 show the variation of the load rectified output voltage sensor and the load current due to positive and negative step change in reference voltage for  $K_p=5$  and  $K_I=0.1$ .



(a) Simulation



(b) Experimental

Fig. 4 Simulation and experimental results for load voltage and current.

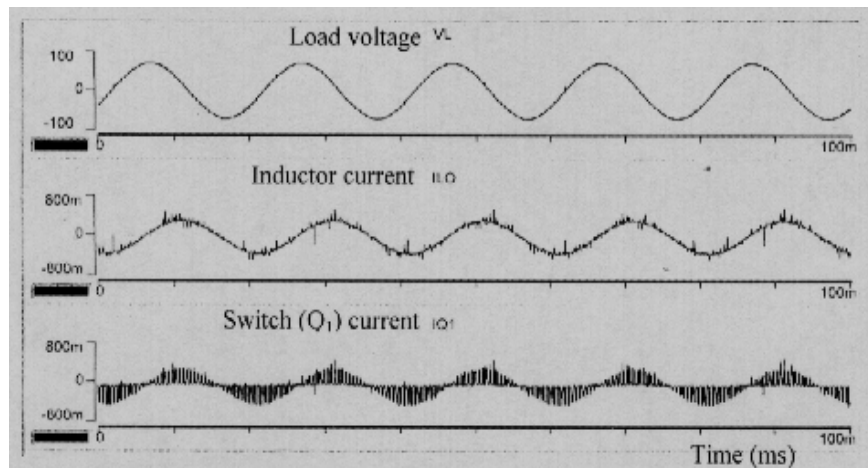


Fig. 5 Experimental waveforms for load voltage, inductor and switch current.

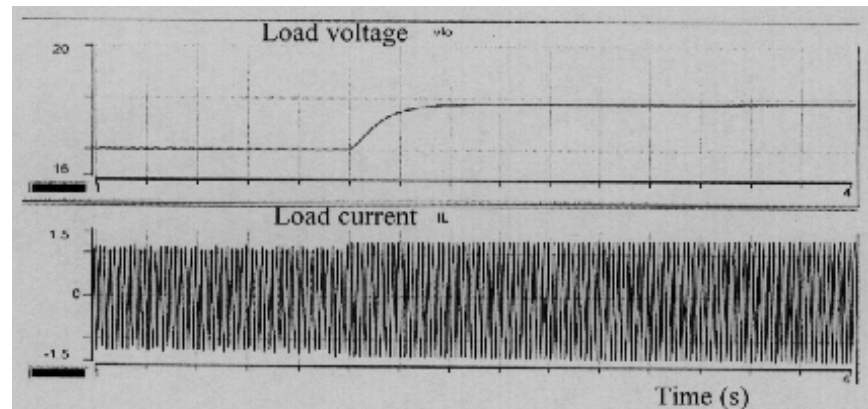


Fig. 6 Variation of the load voltage and current due to a positive step change in reference voltage

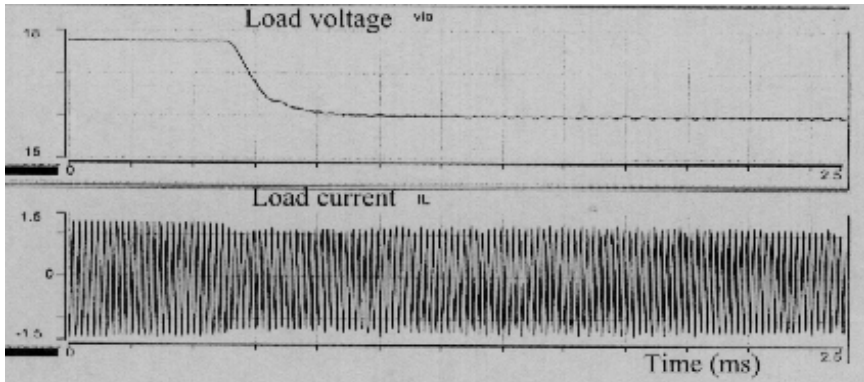


Fig. 7 Variation of the load voltage and current due to a negative step change in reference voltage

#### 4.2.2. Load change

Figure 8 shows the variation of the rectified load output voltage sensor, the control voltage and the load current due to positive and negative load change ( $K_p=5$ ,  $K_i=0.1$ ).

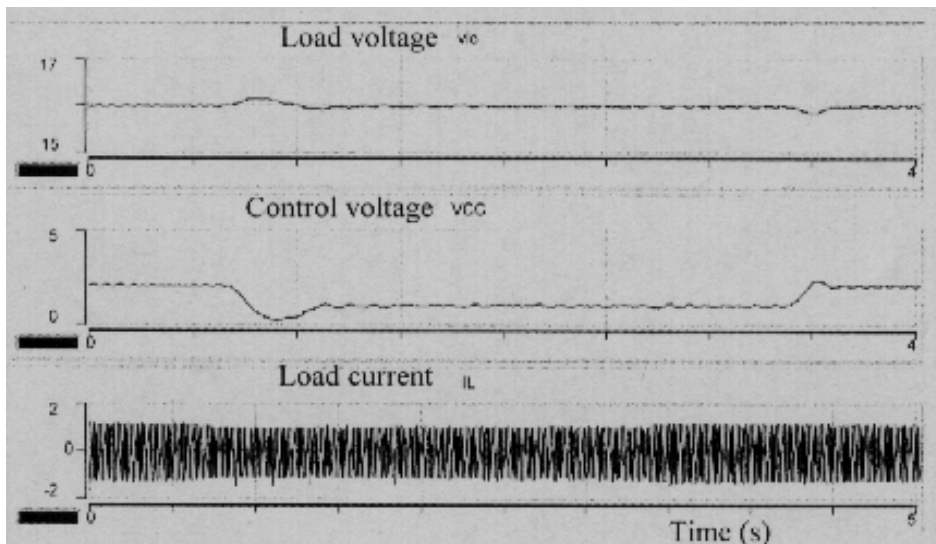


Fig. 8 Variation of load voltage and control voltage due to positive and negative load change

#### 4.2.3. Open and closed loop Run-up for the Universal motor:

Figures 9 and 10 show open and closed loop run-up behavior of the universal motor as a dynamic load with the PI controller. It is observed that the run-up time for closed loop system is decreased and the common coupling bus bar voltage remains constant.

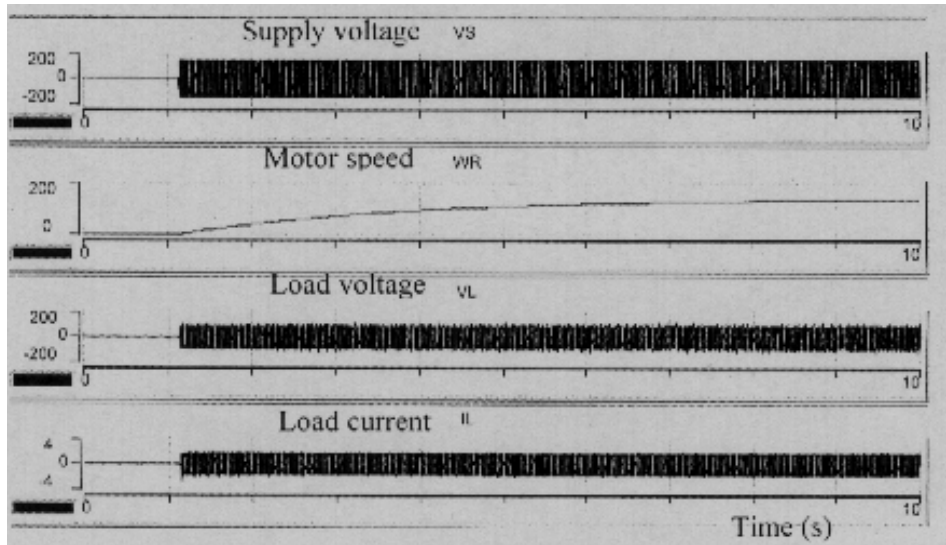


Fig. 9 Open loop run-up behavior for half load

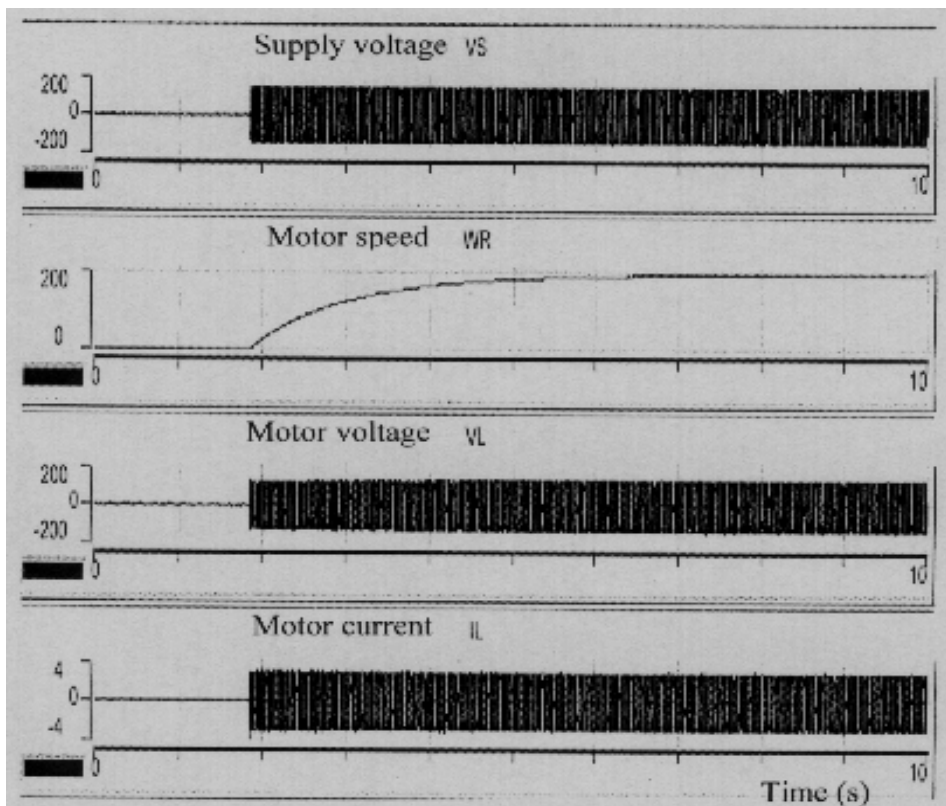


Fig. 10 Closed loop run-up behavior for half load and  $V_{ref}=140$  V.



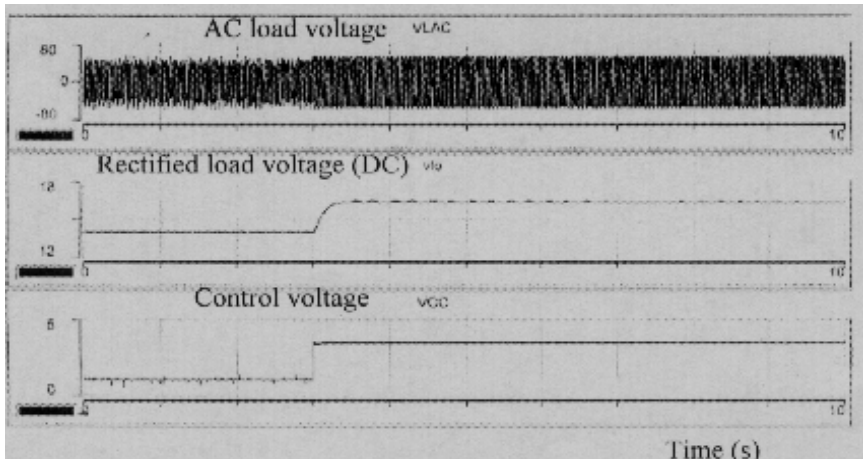


Fig. 11 Responses due to positive step change in reference voltage

### 4.3. Closed loop fuzzy logic controller

The effectiveness of the proposed fuzzy logic controller on the transient and dynamic characteristics of the load voltage stabilization is investigated.

#### 4.3.1. Reference voltage step change for static load

Figures 11 and 12 show the responses of the common coupling bus-bar rectified load output voltage sensor, and the control voltage due to positive and negative step change in the reference voltage for closed-loop fuzzy control system. It is noticed that the response is faster than the PI controller.

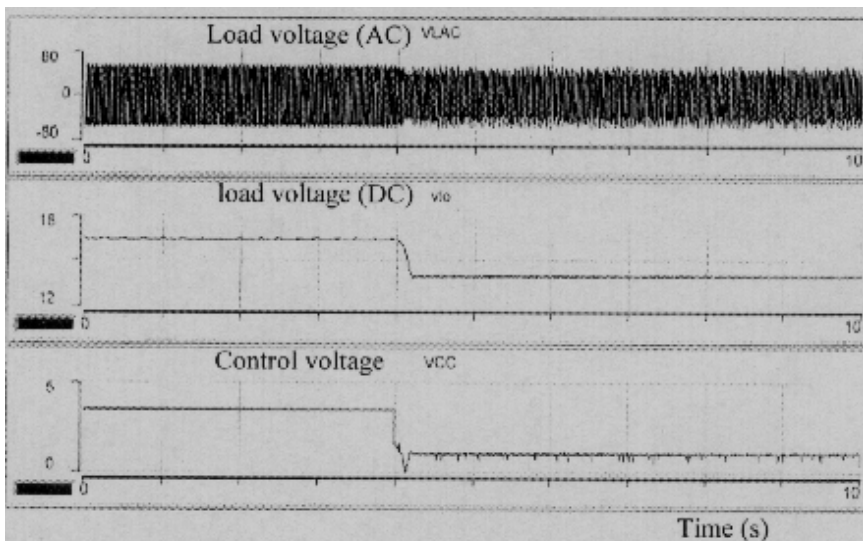


Fig. 12 Responses due to negative step change in reference voltage

#### 4.3.2. Static load change

Figures 13 shows the response of the common coupling bus-bar rectified load voltage sensor, load current and control voltage due to positive and negative load change for closed-loop voltage stabilization using fuzzy control system. It is clear that the response with fuzzy control is faster than with the PI controller and the load voltage is constant.

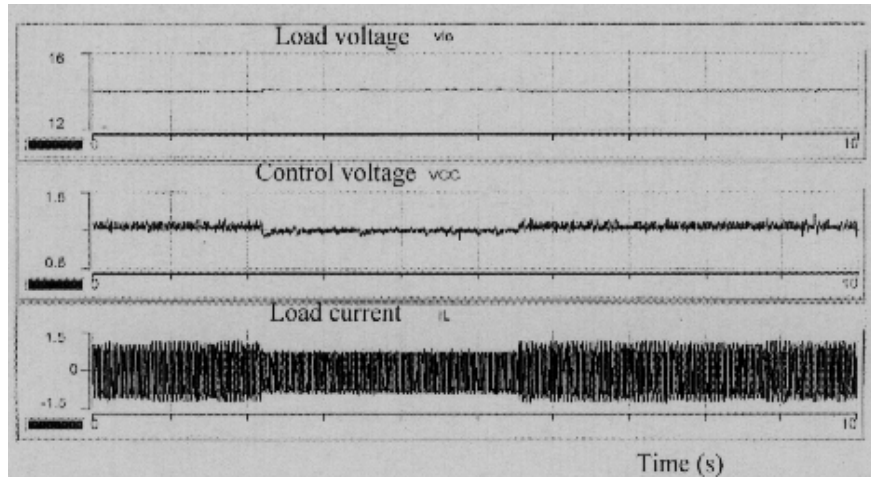


Fig. 13 Variations of load current, load voltage and control voltage due to positive and negative load change for closed loop fuzzy control.

#### 4.3.3. Motor run-up using fuzzy control

Figure 14 shows the waveforms of the motor current, the motor voltage and the motor speed during run-up at half-load and  $V_{ref} = 120$  V for closed loop voltage stabilization using fuzzy logic control. It is observed that the response time is faster than when using the PI controller.

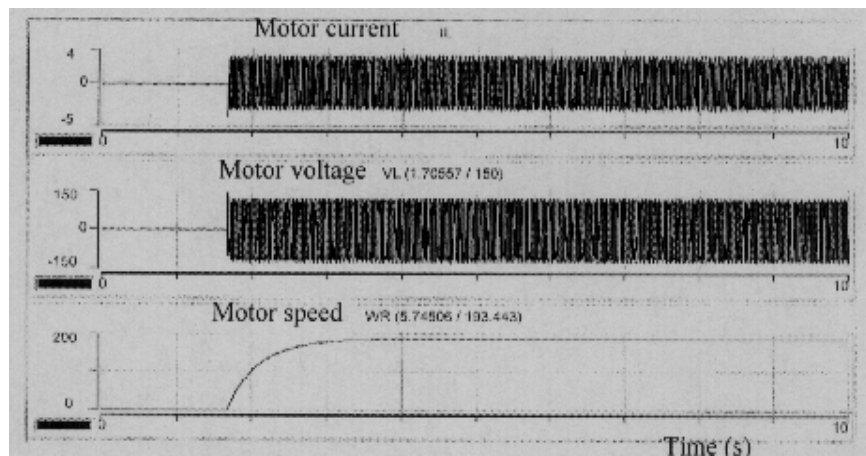


Fig. 14 Run-up behavior for half-load for closed loop voltage stabilization using fuzzy control

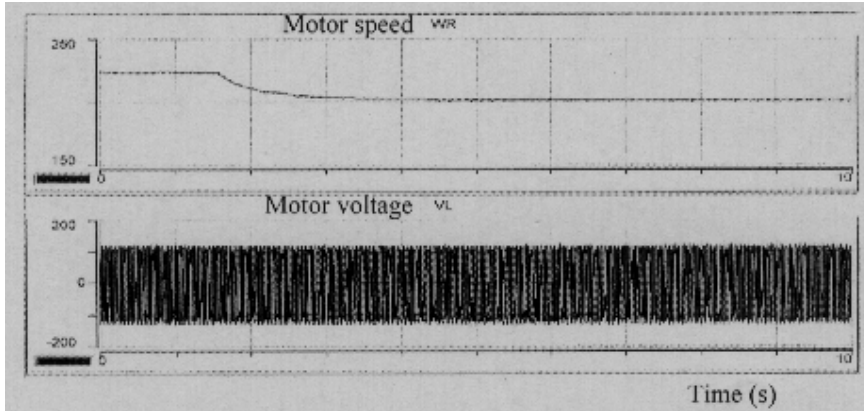


Fig. 15 Response due to a negative change in load torque using fuzzy control.

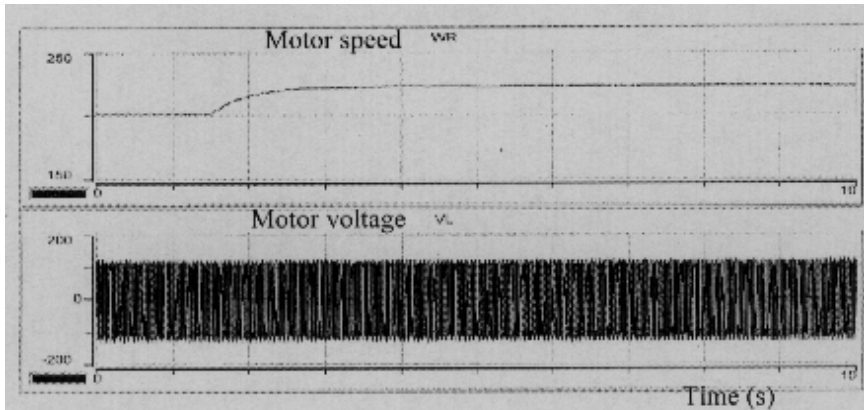


Fig. 16 Response due to a positive change in load torque using fuzzy control.

#### 4.3.4. Dynamic load change

Figures 15 and 16 show the motor voltage and speed response due to positive and negative change in load torque with  $V_{ref} = 120$  V using fuzzy control. It is clear that the load voltage is constant and the time response is faster than when using the PI controller.

## 5. CONCLUSION

A simplified PWM control technique is proposed with switched reactor in parallel with a capacitor for static VAR compensation. The proposed technique is for load voltage stabilization, reactive power compensation and power factor improvement in the presence of feeder impedance. Suitable parameters of the designed system are selected. The load terminal voltage, the load current and the supply current are shown to be close to the sinusoidal form.

The proposed system is fully controlled using the digital signal processor board. The proportional integral voltage controller parameters are given to stabilize the common coupling bus-bar voltage. Moreover, the experimental study using DSP clearly indicates the superior performance of fuzzy logic control for static and or dynamic load. This is because, it is inherently adaptive in nature. By good choice of control parameters, the fuzzy controller can give better

results than the PI controller. Fuzzy control of the complete system gives good response in both motor run-up and during disturbances.

## REFERENCES

- [1] S. Y. Lee, C. J. Wu, and W. N. Chang, "A Compact Control Algorithm For Reactive Power Compensation And Load Balancing With Static VAR Compensator," *Electric Power Systems Research*, Vol. 58, No. 2, pp. 63-70, 2001.
- [2] P. K. Shadhu Khan, and J. K. Chatterjee, "Operational Capability Of Inductively Loaded Current Controlled Solid-State Lead-Lag VAR Compensator, *International Journal of Electrical Power & Energy Systems*, Vol. 25, No. 4, pp. 275-292, 2003.
- [3] C. S. Chang, and Y. Qizhi, "Fuzzy Bang-Bang Control Of Static VAR Compensators For Damping System-Wide Low-Frequency Oscillations," *Electric Power Systems Research*, Vol. 49, No. 1, pp. 45-54, 1999.
- [4] H. Rastegar, M. Abedi, M. B. Menhaj, and S. H. Fathi, "Fuzzy Logic Based Static VAR Compensators For Enhancing The Performance of Synchronous And Asynchronous Motor Loads," *Electric Power Systems Research*, Vol. 50, No. 3, pp.191-204, 1999.
- [5] L. Moran, P. D. Ziogas, and G. A. Joos, "A Solid-State High-Performance Reactive-Power Compensator," *IEEE Transaction on Industry Application*, Vol. 29, No. 5, pp. 969-978, 1993.
- [6] C. R. Vidyashankar, and A. K. Khargekar, "A Practical Fast Acting Control Scheme For Static VAR Compensator," *Electric Machines and Power Systems*, No. 1, pp. 357-366, 1986.
- [7] G. Joos, L. Moran, and P. D. Ziogas, "Performance Analysis of a PWM Inverter VAR Compensator," *IEEE Transaction on Power Electronic*, Vol. 6, No. 8, pp. 380-391, 1991.
- [8] S. E. Haque, N. H. Malik, and W. Shepherd, "Operation of a Fixed Capacitor-Thyristor Controlled Reactor (FC-TCR) Power Factor Compensator," *IEEE Transaction on Power Apparatus and Systems*, PAS-104, No. 6, pp. 1385-1390, 1985.
- [9] J. B. Ekanayake, N. Jenkins, and C. B. Cooper, "Experimental Investigation of an Advanced Static VAR Compensator," *IEE Proceeding General Transmission Distribution*, Vol. 142, No. 2, pp. 202-210, 1995.
- [10] H. Jin, G. Goos, and G. Lopes, "An Efficient Switched-Reactor Based Static VAR Compensation," *IEEE Transaction on Industry Application*, Vol. 30, No. 4, pp. 998-1005, July/Aug. 1994.
- [11] A. A. Amin, "A Three-phase Four-Wire Advanced Static VAR Compensator," *International Middle-East Power Systems Conference (MEPCON'2000)*, Cairo, Egypt, pp. 44-48, March 28-30, 2000.
- [12] A. M. Sharaf, M. Z. El-Sadek, F. N. Abd-Elbar, and A. M. Hemeida, "A Novel Error Driven Nonlinear Control Strategy For Transient Stability Enhancement Using Static VAR Compensators," *International Middle-East Power Systems Conference (MEPCON'2000)*, March 28-30, Cairo, Egypt, pp. 223-227, 2000.

## Nomenclature

- C: Compensator capacitor,  $\mu\text{F}$   
F: Motor viscous friction coefficient,  $\text{N.m/r/s}$ .  
 $I_s, i_s$ : R.M.S. and instantaneous supply current, A  
 $L_s$ : Supply inductance, H  
 $L_\theta, L_l$ : Controlled coil and load inductance's, H  
 $R_\theta, R_l$ : Controlled coil and load resistance's, ohm  
 $R_s$ : Supply resistance, ohm  
 $V_s, v_s$ : R.M.S. and instantaneous supply voltage, V

$V_m, v_m$ : R.M.S. and instantaneous load terminal voltage, V

$Z_L$  : Load impedance, ohms

$\phi_l$ : Load phase- angle

$\omega$ : Angular frequency

$L_a, L_f$ : The armature and field of the motor inductance's, H

$R_a, R_f$ : The armature and field of the motor resistance's, ohm

J: The moment of inertia,  $\text{kg.m}^2$

$T_e, T_l$ : The electromagnetic and the load torque, N.m

$K_p$ : Proportional gain

$K_i$ : Integral gain

Appendix

The parameter values of the designed system at 50 Hz are as follows:

$$R_l = 25 \text{ ohm} \quad L_l = 0.159 \text{ H}$$

$$R_\theta = 2.5 \text{ ohm} \quad L_\theta = 0.199 \text{ H}$$

$$R_s = 2.5 \text{ ohm} \quad L_s = 0.027 \text{ H}$$

$$C = 55 \text{ } \mu\text{F}$$

The test motor data and parameters:

$$1/3 \text{ HP, } 220 \text{ V, } 1.9 \text{ A, } 6000 \text{ r/min}$$

Universal motor has the following measured parameters:

$$R_a + R_f = 13.7 \text{ ohm,} \quad L_a + L_f = 0.169 \text{ H,}$$

$$F = 0.00012 \text{ N.m/r/s,}$$

$$J = 0.003 \text{ kg.m}^2$$